

Axial Turbulent Diffusion in Fluid between Rotating Coaxial Cylinders

Y. Enokida
K. Nakata
A. Suzuki

Department of Nuclear Engineering
University of Tokyo
Tokyo, 113 Japan

The viscous flow between a long stationary outer cylinder and a coaxial rotating inner cylinder takes place along circular stream lines (Couette flow) if a suitable dimensionless measure of the inner rotation speed, i.e., the Taylor number, is small enough. When the Taylor number exceeds a critical value, vortices appear, periodically spaced in the axial direction (Taylor vortex flow). When the Taylor vortex flow is associated with a flow in the axial direction, a spiral flow is induced. The rotary annular column with a spiral flow has been used as an extractor on a laboratory scale for over 50 years (Lo et al., 1982). However, the mass transport phenomena have been scarcely investigated, and the uncertainty associated with the radial scale-up effect on the extraction efficiency makes it difficult to use the rotary annular column for industrial purposes.

Recently, Tam and Swinney (1987) studied mass transport experimentally in the turbulent Couette-Taylor flow without an axial flow, using a relatively small-scale apparatus, the annular gap-width of which ranged from 1.285 to 0.318 cm. They proposed a one-dimensional model for the analysis of mass transport and measured the effective axial diffusion coefficient, i.e., the axial dispersion coefficient, \tilde{D} , for radius ratios, η , ranging from 0.494 to 0.875, and at Reynolds numbers, Re_θ , ranging from 50 to 1,000 times the onset of Taylor vortex flow. They described the dispersion coefficient by a power law, $\tilde{D} \propto Re_\theta^\beta$, whose β varies upon the experimental conditions and geometry of an experimental apparatus.

The objectives of this work are the following:

- Discussion of the scale-up effect on axial mixing by the measurement of axial dispersion coefficients, using the experimental apparatus of larger rotating coaxial cylinders
- Development of a general correlation for the axial dispersion coefficients in rotating coaxial cylinders under several operational conditions
- Measurement and discussion of axial dispersion coefficients with an axial flow

Experimental Methods

Rotating coaxial cylinders

A schematic diagram of the experimental apparatus is shown in Figure 1, and the characteristic dimensions of the two columns are summarized in Table 1. The outer cylinder, made of borosilicate glass, was fixed, and the inner cylinder, made of stainless steel, was rotated by a stepping motor. The rotation rate ranged from 30 to 200 revolutions per minute, which was controlled by an electric pulse generator. The effective length of the annulus, L , was 40 or 50 cm, and the aspect ratios, $\Gamma = L/d$, where d is the gap between the cylinders, were 22.2 or 16.4. To minimize the influence of the top boundary on the axial dispersion process, the axial length of the upper settling part was 40 cm in excess of the effective height of the annulus.

Deionized water was used as testing fluid for the measurement of dispersion coefficients. Deionized water was contained in a stainless steel tank of 0.1 m³ in volume and pumped to the experimental apparatus at a constant flow rate. The linear flow velocity ranged from 0 (i.e., Couette-Taylor condition) to 1.16 cm · s⁻¹ (at maximum axial flow rate). All experiments were performed at room temperature (289 K), and the temperature deviation was measured before and after each run. The maximum temperature rise was within 1 K, so the joule heating due to rotation of the inner cylinder was negligible. Effluent from the column was drained through the outlet line to a receiver tank.

The stepping motor began rotating when the system was filled with fluid. Thereafter, equilibrium flow patterns were reached in a few minutes.

Measured method

Dye solution (0.63 mol · dm⁻³ methylene blue; C₁₆H₁₈N₃ClS · 4H₂O) was injected by a micro tubing pump approximately 0.01 cm³ · s⁻¹ through a stainless steel tube (0.125 mm ID) located in the middle of the settling down region. The dye concentration was determined as a function of

Correspondence concerning this paper should be addressed to Y. Enokida.

time by laser absorption measurements. A single helium-neon laser (1 mW) was scanned along the outer cylinder by a linear-gear motor for the measurement of dispersion coefficient when there was no axial flow. The scanning width was 19 cm, and the scanning frequency was 0.1 Hz. Double beams at fixed positions were used to measure dispersion coefficients with an axial flow. The beam from a helium-neon laser was directed through the gap between the cylinders in both methods. The transmitted laser intensity, monitored with a photodiode, was recorded as a function of time in the computer system.

After each measurement, a small amount of flow visualization particles was introduced into the fluid, so that we could observe the flow pattern. The number of Taylor vortices was counted at that point, to obtain the average axial wavelength, λ , for the fluid without an axial flow rate. The experimental system was flushed with deionized water several times after each measurement before the next run.

Analytical Model

The transport of species A , e.g., dye, with concentration, $C_A(\vec{r}, t)$, in an incompressible flow is governed by

$$\frac{\partial C_A(\vec{r}, t)}{\partial t} + \vec{v}(\vec{r}, t) \cdot \nabla C_A(\vec{r}, t) = D_{\text{mol}} \nabla^2 C_A(\vec{r}, t), \quad (1)$$

where $\vec{v}(\vec{r}, t)$ is the fluid velocity and D_{mol} is the molecular diffusion coefficient. This equation can be simplified to a one-dimensional diffusion equation for Taylor vortex flow because the following conditions are satisfied (Tam, 1987):

- The fluid is well mixed in both the radial and azimuthal directions on a time scale that is short compared to that for axial transport.

- The transport process is measured with a length scale that is large compared to the size of the largest eddies.

We applied the same simplification not only for Taylor vortex flow, but also for the spiral flow. A one-dimensional form for Eq. 1 is

$$\frac{\partial C_A(z, t)}{\partial t} + v_z \cdot \frac{\partial C_A(z, t)}{\partial z} = \tilde{D} \frac{\partial^2 C_A(z, t)}{\partial z^2} \quad (2)$$

where z is the coordinate along the axial of rotation and $C_A(z, t)$ is the concentration of species A , averaged in the radial and azimuthal directions and over an axial distance on the order of vortex size.

The assumptions that allow Eq. 1 to be written as Eq. 2 are examined by the preliminary scanning measurement of concentration flatness in a Taylor vortex in the axial direction at the top boundary of the measuring region (19 cm), because a circular stream line takes place in the vertical cross section of a single vortex.

Since the measuring region is relatively small compared to the total length of the column (160 cm) in our experimental apparatus, we can ignore the end effects and have taken the mathematical model proposed by Aris (1959) and Bischoff (1960, 1962), which can also be adopted to a scanning measurement (where a laser and a detector are moving with v_z^*) by changing the variable, $z^* = z + v_z^* \cdot t$, where z^* is the position which the laser beam reaches at time t . The effective dispersion coefficient in the Peclet number ($Pe = v_z L_0 / \tilde{D}$ or $v_z^* L_0 / \tilde{D}$) is evaluated by the

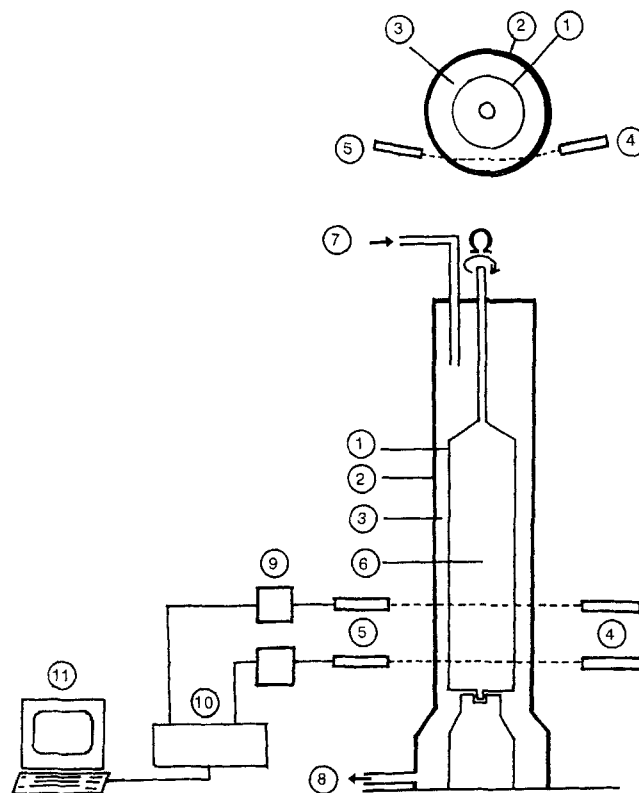


Figure 1. Experimental apparatus.

- | | |
|-------------------|---------------------|
| 1. Inner cylinder | 7. Feed solution |
| 2. Outer cylinder | 8. Effluent |
| 3. Annulus | 9. Amplifier |
| 4. He-Ne laser | 10. A/D converter |
| 5. Photodiode | 11. Computer system |
| 6. Dye injector | |

difference of the variance ($\Delta\sigma^2$) of the normalized concentration curve as a function of time, using the following relationship (Aris, 1959; Bischoff, 1962):

$$\Delta\sigma^2 = \frac{2}{Pe} \quad (3)$$

Results and Discussion for Taylor-Couette Flow

Dependence of rotation speed on axial dispersion coefficients

The measured values of the axial dispersion coefficients, \tilde{D}_0 , without axial flow are typically $0.1 \sim 0.5 \text{ cm}^2 \cdot \text{s}^{-1}$, which are more than four orders of magnitude larger than the molecular diffusion coefficient. This means that vortices of various scale greatly enhance mass transport in a rotating coaxial extractor.

\tilde{D}_0 at each radius ratio increased continuously with rotary speed, as shown in Figure 2. \tilde{D}_0 can be described by a power law

Table 1. Parameters for Experimental Apparatus

	Inner Dia. r_1 cm	Outer Dia. r_2 cm	Gap Width d cm	Dia. Ratio η	Effect. Height L cm	Aspect Ratio Γ
Column I	4.45	7.50	3.05	0.593	50	16.4
Column II	5.70	7.50	1.80	0.760	40	22.2

in rotation speed, i.e., the Reynolds number in the azimuthal direction. Tam and Swinney (1987) proposed the following relationship:

$$\tilde{D}_0 = \frac{\lambda}{2d} \tilde{D}_0^* \left(\frac{Re_\theta}{Re_\theta^c} \right)^\beta \quad (4)$$

where Re_θ^c was the critical value at the bifurcation point between the Couette and Taylor vortex flows. We also tried a similar correlation, but the best values of \tilde{D}_0^* and the exponent β for our data did not agree with the previous observations by Tam and Swinney (1987). This was because our experimental apparatus had an approximately three times larger diameter of the outer cylinder than was used in the prior study, while the radius ratio was almost same.

Scale effect on axial dispersion coefficients

According to the analysis of the hydrodynamic instability, as the gap width increases, the revolution rate lowers, to which the flow is critical in becoming a vortex flow (Taylor, 1923). Therefore, the strength of the vortex is influenced by a geometrical factor.

We visualized Taylor vortex flow by the addition of small particles to observe stream lines in the gap of the column. Judging from the observation, convection dominated the transport within the Taylor vortex, similarly to the Rayleigh-Bénard convection cell (Shraiman, 1987). Therefore, the concentration gradient, between adjacent stream lines within the Taylor vortex, averages out to almost zero. On the other hand, in the vicinity of the separatrix between the vortices, the vertical component of the flow velocity vanished and the mechanism of the mass transport from one vortex to another was mainly by diffusion through the separatrix zone. In our observation, increasing the rotation speed of the inner cylinder increased the frequency with which small particles went through this zone. We therefore conclude that the strength of the vortex dominates the mass transport pro-

cess near the separatrix. As a measure of the strength of the Taylor vortex, we selected $r_m \Omega^2$, which is used by Davis, Jr., and Weber (1960), to analyze data on hold-up fraction in a liquid-liquid extractor. Figure 3 illustrates the correlation between the measured data for effective dispersion coefficients and the strength of the vortex. Therefore, the behavior of the dispersion coefficient is described well by the following equation:

$$\tilde{D}_0 = \alpha (r_m \Omega^2)^\beta \quad (5)$$

where $\alpha = 0.0309$ and $\beta = 0.405$.

In Figure 3, the data obtained by other investigators are plotted in addition to our experimental data, and both kinds of data are well correlated. This result is of practical importance for a design study of this type of extractor.

Results and Discussion for Spiral Flow

Axial wavelength

Flow in the axial direction in the gap of the coaxial cylinders caused a pair of stable counter-rotating spiral flows. We measured the averaged pitch, λ , of the spiral flow. In the Taylor vortex flow, the wave number, a , was defined by the following equation:

$$a = \frac{2\pi}{\lambda} d. \quad (6)$$

And a is almost equal to the critical wave number ($a_c = 3.12$) that is given at the occurrence of the Taylor vortex (Chandrasekhar, 1961). In our experimental region, all wavenumbers calculated by using Eq. 6 agreed very closely with a_c , and the average pitch of the vortex was scarcely affected by the axial flow.

Effect of flow rate on axial dispersion coefficients

A convective flow enhances the dispersion in general. In spiral flow through the gap between rotating coaxial cylinders, turbulent mixing along the helical axis of the flow is added to the diffusion through the separatrix zone. Since the azimuthal component of flow velocity is characterized by $Re_\theta v_z$, the ratio $(\tilde{D} - \tilde{D}_0)/(r_i \Omega d)$ should be proportional to the axial velocity, v_z . Figure 4 shows this proportionality for all measured data of

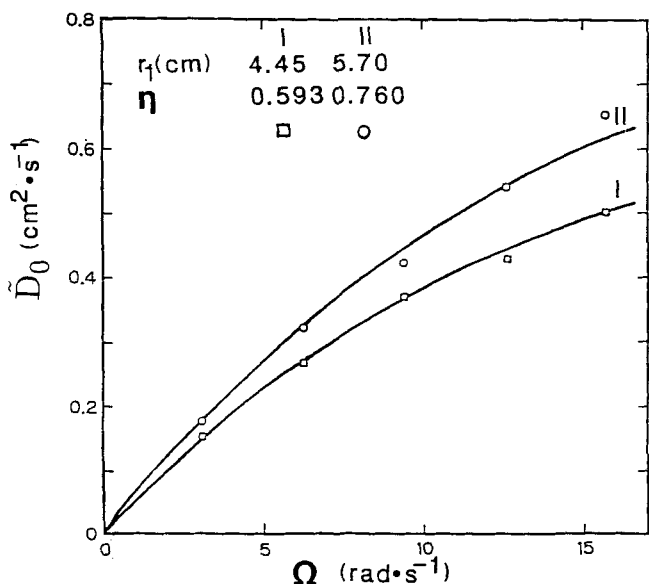


Figure 2. Measured values of dispersion coefficient, \tilde{D}_0 .
Experimental data = function of angular velocity.

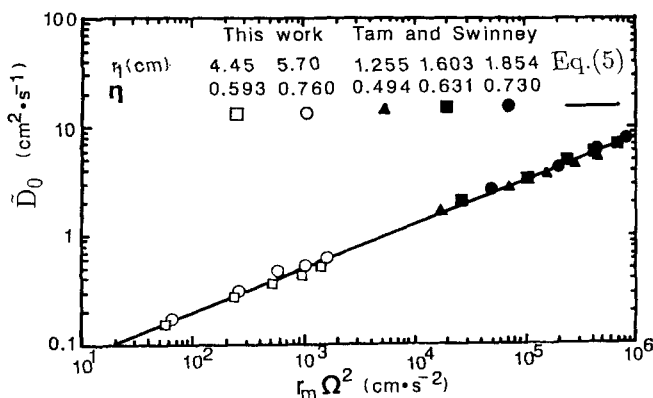


Figure 3. Dispersion coefficients: this study vs. others with general correlation.

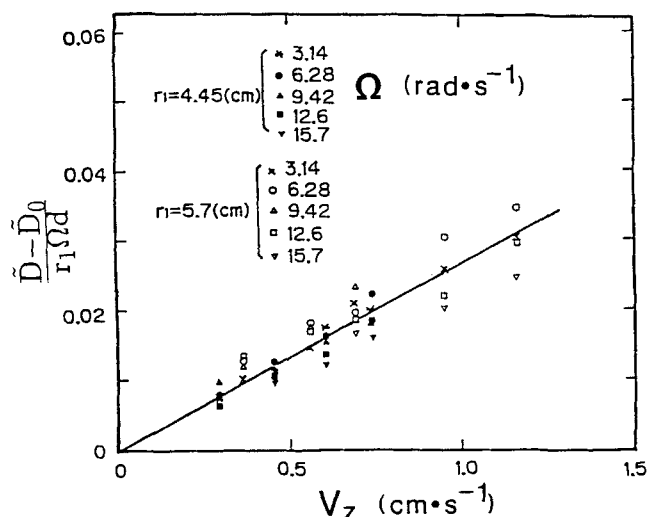


Figure 4. Effect of axial flow velocity on dispersion coefficient.

\tilde{D} . This relation describes each data with an error of approximately $\pm 25\%$, so that the following equation can be used to evaluate the dispersion coefficient for a flow of deionized water in the rotating coaxial cylinders:

$$\tilde{D} = \alpha(r_m \Omega^2)^\beta + \gamma r_1 \Omega d v_z, \quad (7)$$

where $\alpha = 0.0309$, $\beta = 0.405$, and $\gamma = 0.027$.

The uncertainty in this correlation increases with an increase in v_z . To reduce the uncertainty, an advanced experiment and a new correlation based on a multi-dimensional convective diffusion model should be tested in future experiments, which should include complicated concentration measurements.

Notation

- a = wavenumber of Taylor vortex, cm^{-1}
- a_c = critical wavenumber of Taylor vortex, cm^{-1}
- $C_A(z, t), C_A(r, t)$ = concentration of component A, mol m^{-3}
- d = gap width between concentric cylinders, cm
- \tilde{D} = dispersion coefficient in axial direction, $\text{cm}^2 \cdot \text{s}^{-1}$
- \tilde{D}_0 = dispersion coefficient in axial direction without axial flow, $\text{cm}^2 \cdot \text{s}^{-1}$
- D_0^* = scaled diffusion coefficient, Tam and Swinney, $\text{cm}^2 \cdot \text{s}^{-1}$
- D_{mol} = molecular diffusion coefficient, $\text{cm}^2 \cdot \text{s}^{-1}$

- L = height of effective experimental region, cm
- L_0 = height of experimental space for measuring effective diffusion coef., cm
- Pe = Peclet number, $v_z L_0 / \tilde{D}$
- Re_θ = Reynolds number in azimuthal direction, $r_1 \Omega d / \nu$
- Re_θ^c = critical Reynolds number in azimuthal direction, $r_1 \Omega d / \nu$
- \vec{r} = position, cm
- r_1 = diameter of inner concentric cylinder, cm
- r_2 = diameter of outer concentric cylinder, cm
- r_m = average diameter $(r_1 + r_2)/2$, cm
- t = time, s
- v_z = linear flow rate in axial direction, $\text{cm} \cdot \text{s}^{-1}$
- v_z^* = velocity of scanning laser, $\text{cm} \cdot \text{s}^{-1}$
- $\vec{v}(r, t)$ = fluid velocity, $\text{cm} \cdot \text{s}^{-1}$
- z = axial coordinate, cm
- z^* = axial coordinate for moving boundary, cm

Greek letters

- α = coefficient in the power law
- β = exponent of the power law
- γ = coefficient in the power law
- η = radius ratio
- ν = kinetic viscosity, $\text{cm} \cdot \text{s}^{-1}$
- λ = averaged wavelength of a Taylor vortex, cm
- $\Delta \sigma^2$ = variance difference of response curve for tracer conc. after injection
- Γ = aspect ratio, L/d
- Ω = angular velocity of inner cylinder, $\text{rad} \cdot \text{s}^{-1}$

Literature Cited

- Aris, R., "Notes on the Diffusion-Type Model for Longitudinal Mixing in Flow," *Chem. Eng. Sci.*, **9**, 266 (1959).
- Bischoff, K. B., "Notes on the Diffusion-Type Model for Longitudinal Mixing in Flow," *Chem. Eng. Sci.*, **12**, 69 (1960).
- Bischoff, K. B., and O. Levenspiel, "Fluid Dispersion- Generalization and Comparison of Mathematical Models: I. Generalization of Models," *Chem. Eng. Sci.*, **17**, 245 (1962).
- Chandrasekhar, S., "Hydrodynamic and Hydromagnetic Stability," Oxford University Press (1961).
- Davis, Jr., M. W., and E. J. Weber, "Liquid-Liquid Extraction between Rotating Concentric Cylinders," *Ind. Eng. Chem.*, **52**, 929 (1960).
- Lo, T. C., M. H. I. Baird, and C. Hanson, "Handbook of Solvent Extraction," John Wiley and Sons, New York (1983).
- Shraiman, B. I., "Diffusive Transport in a Rayleigh-Bénard Convection Cell," *Physical Rev. A*, **36**, 261 (1987).
- Taylor, G. I., "Stability of a Viscous Liquid Contained between Two Rotating Cylinders," *Phil. Trans. Roy. Soc. Lond., A*, **223**, 289 (1923).
- Tam, W. Y., and H. L. Swinney, "Mass Transport in Turbulent Couette-Taylor Flow," *Physical Rev. A*, **36**, 1374 (1987).

Manuscript received Oct. 13, 1988, and revision received Apr. 11, 1989.